Amphawan et al. EURASIP Journal on Wireless Communications and Networking 2012, 2012:356
http://jwcn.eurasipjournals.com/content/2012/1/356

EURASIP Journal on Wireless Communications and Networking
a SpringerOpen Journal

RESEARCH Open Access

An integrated priority-based cell attenuation model for dynamic cell sizing

Angela Amphawan*, Mohd Nizam Omar and Roshidi Din

Abstract

A new, robust integrated priority-based cell attenuation model for dynamic cell sizing is proposed and simulated using real mobile traffic data. The proposed model is an integration of two main components; the modified virtual community–parallel genetic algorithm (VC-PGA) cell priority selection module and the evolving fuzzy neural network (EFuNN) mobile traffic prediction module. The VC-PGA module controls the number of cell attenuations by ordering the priority for the attenuation of all cells based on the level of mobile level of mobile traffic within each cell. The EFuNN module predicts the traffic volume of a particular cell by extracting and inserting meaningful rules through incremental, supervised real-time learning. The EFuNN module is placed in each cell and the output, the predicted mobile traffic volume of the particular cell, is sent to local and virtual community servers in the VC-PGA module. The VC-PGA module then assigns priorities for the size attenuation of all cells within the network, based on the predicted mobile traffic levels from the EFuNN module at each cell. The performance of the proposed module was evaluated on five adjacent cells in Selangor, Malaysia. Real-time predicted mobile traffic from the EFuNN structure was used to control the size of all the cells. Results obtained demonstrate the robustness of the integrated module in recognizing the temporal pattern of the mobile traffic and dynamically controlling the cell size in order to reduce the number of calls dropped.

Keywords: Dynamic cell sizing, Mobile traffic prediction, Cell priority selection, Resource management

1. Introduction

Traffic congestion control is a key issue in high-speed cellular networks. Rapidly increasing demands for high network bandwidth, driven by real-time multimedia traffic, have stimulated research on various traffic congestion control schemes [1-9]. Dynamic cell sizing is a traffic congestion control mechanism which increases the capacity of a network by varying the pilot power to modify the coverage area of cells adaptively for optimum performance under various traffic loads [10-17]. The dynamic cell sizing mechanism attempts to keep the forward and reverse link handoff boundaries balanced by changing the forward link coverage according to the changes in the reverse link interference level [17,18]. During heavy traffic, dynamic cell sizing is able to increase the capacity of the forward link by delegating the traffic from overloaded cells to adjacent uncongested cells in order to promote optimum utilization of the pilot power. Nevertheless, a dynamic cell sizing environment is known to suffer from the occurrence of coverage holes, where calls are dropped and the quality of service may not be maintained [16,19]. In order to mitigate the occurrence of coverage holes, a new integrated priority-based cell attenuation model (IPCAM) for dynamic cell sizing is proposed. The proposed model is an integration of two main components; the modified virtual community–parallel genetic algorithm (VC-PGA) cell priority selection module [16] and the evolving fuzzy neural network (EFuNN) mobile traffic prediction module. The EFuNN module is placed in each cell within the network and the predicted mobile traffic volume of each cell is sent to the local and VC servers in the VC-PGA module. The VC-PGA module then assigns priorities for the size attenuation of all cells within the network, based on the predicted mobile traffic levels from the EFuNN module at each cell.

As a foundation, the basic principles of dynamic cell sizing are reviewed in Section 2, leading to the motivation for the new IPCAM. For a holistic understanding of

* Correspondence: angela@uum.edu.my
Internetworks Research Laboratory, School of Computing, Universiti Utara Malaysia, Sintok, Kedah 06010, Malaysia

© 2012 Amphawan et al.; licensee Springer. This is an Open Access article distributed under the terms of the Creative Commons Attribution License (http://creativecommons.org/licenses/by/2.0), which permits unrestricted use, distribution, and reproduction in any medium, provided the original work is properly cited.

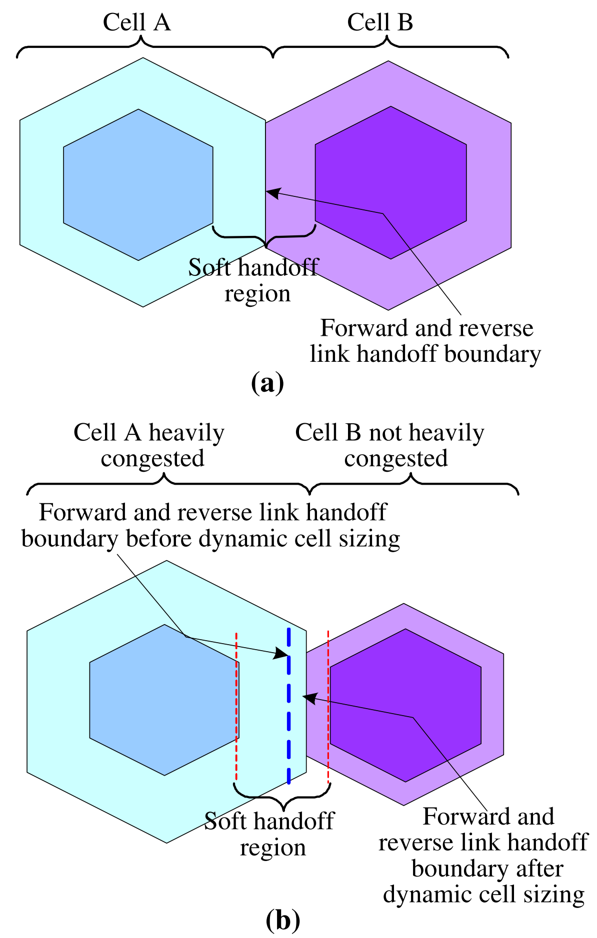

Figure 1 Handoff boundary has moved closer to Cell B due to loading on Cell A. (a) before cell attenuation **(b)** after cell attenuation.

the framework and operation of the new IPCAM, it is necessary to first describe the main constituting components. The VC-PGA module is described in Section 3 while the EFuNN module placed at each cell is described in Section 4. The framework of the new IPCAM is then presented in Section 5. The performance of the IPCAM in controlling the number of coverage holes is evaluated through simulations of a dynamic cell sizing environment using real mobile traffic data. These simulations are described in Section 6, including the results, and the conclusions are drawn in Section 7.

2. Dynamic cell sizing

2.1. Dynamic cell sizing mechanism

The dynamic cell sizing mechanism strives to keep the forward and reverse link handoff boundaries in equilibrium by changing the forward link coverage according to the changes in the reverse link interference level [17,18]. The reverse link handoff boundary is the contour of mobile locations between adjacent cells where the received signal-to-noise ratio (SNR) at the two base stations is the same whereas the forward link handoff boundary is defined as the contour of location where the ratio of the received pilot chip energy of the cell to the spectral density of the total interference seen by the mobile is the same. Thus, if the interference levels are the same at both adjacent base stations and the same amount of power is transmitted on the pilot channel from each base station, then the forward and reverse handoff boundaries will coincide, as shown in Figure 1a. The boundary will exactly be midway between the two cells for a uniform propagation model.

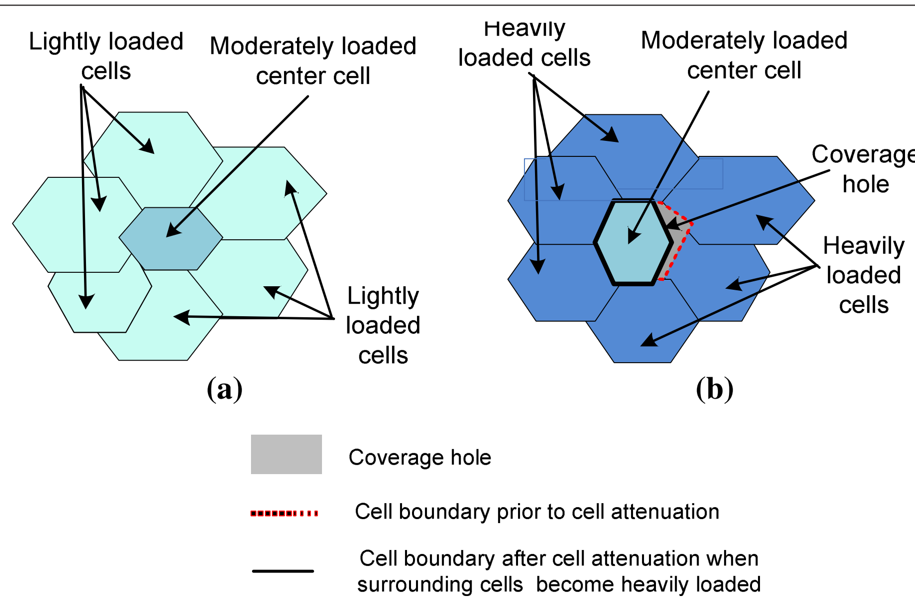

Figure 2 The inevitable development of coverage holes in a dynamic cell sizing environment in an attempt to accommodate increasing traffic in surrounding cells: (a) before cell attenuation; (b) after cell attenuation.

As the reverse link traffic load is increased, the thermal noise at the base station increases. To balance the SNR between the two adjacent base stations, the reverse link handoff boundary will move closer to the base station which has a larger increase in thermal noise. Then, to compensate for the change in the reverse link boundary, the pilot signal of the cell with greater base station interference will be reduced so that the ratio of the received pilot chip energy of the cell to the spectral density of the total interference seen by the mobile is the same.

2.2. Impact of pilot signal of a single cell on forward link performance

Dynamic cell sizing is able to increase the capacity of the forward link by shedding the traffic of overloaded cells to neighboring cells. Consider the case where Cell A in Figure 1b is heavily congested and Cell B is not. In order to move the handoff boundary by an equal amount that the interference has risen in a cell, the dynamic cell sizing algorithm will introduce an attenuation equal on the forward link of Cell A in response to a rise over thermal noise in the reverse link of Cell A [17]. When the handoff boundary is moved closer to Cell B, the first users that are inside Cell B and are in soft handoff with Cell A may fall out of soft handoff with Cell A, relieving some capacity from Cell A to be used for users that are inside Cell A. The second advantage of dynamic cell sizing is that the traffic channel forward gains will increase by the same amount as the cell sizing attenuation, until the total traffic channel power leaving the cell becomes close to the initial value prior to cell size reduction. The output power after cell sizing will be less due to lower power on overhead channels, assuming overhead channels are not power controlled. The reduction of total transmit power due to reduced power on the overhead channels will eventually be used by new users and therefore the total transmit power will remain unchanged before and after cell sizing under heavy traffic conditions [17].

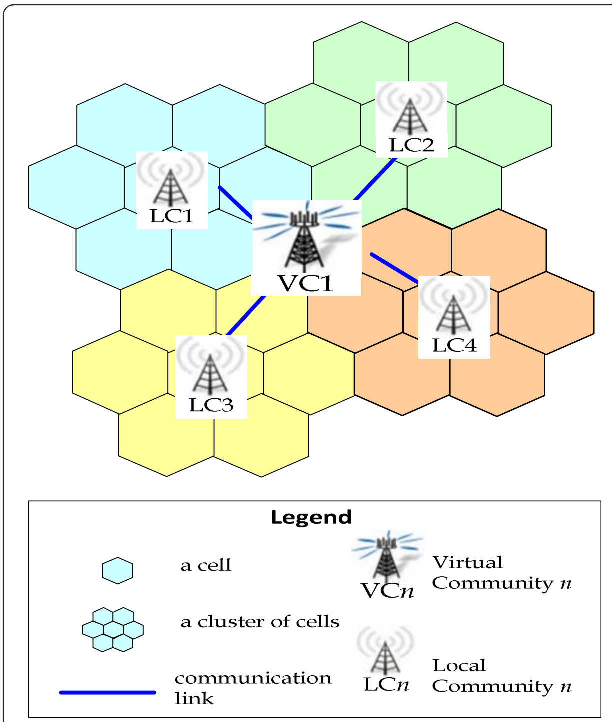

Figure 3 Diverse cell interaction—VC-PGA module for dynamic cell sizing [9].

2.3. Diverse cell interactions in a dynamic cell sizing environment

In Section 2.2, the effect of the change in the pilot power for a single cell was described. This reverse link balancing mechanism is applicable to any cell within the network. Thus, the cell whose size is being controlled may

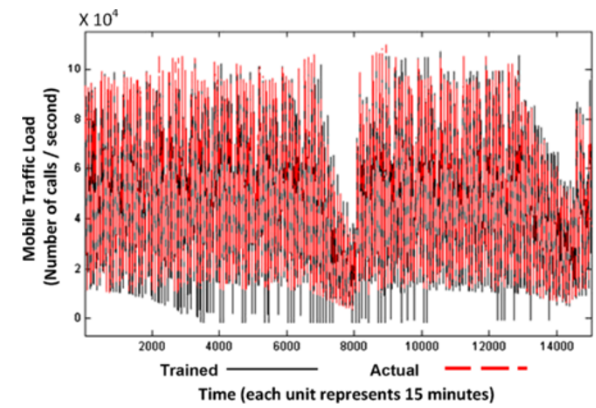

Figure 4 Training of previous half-year's data traffic load for the prediction of the following half-year's data traffic load.

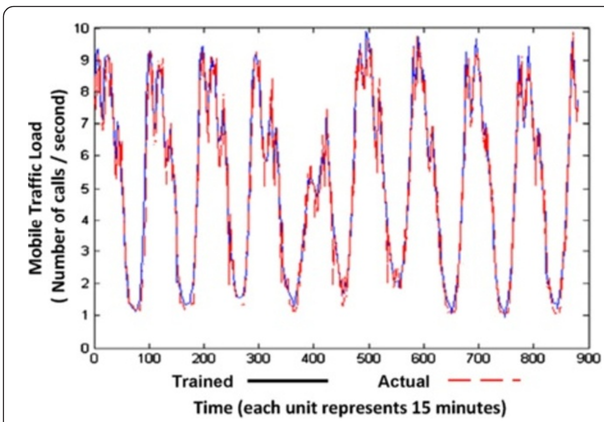

Figure 5 Training of previous half-year's data traffic load for the prediction of the following half-year's data traffic rates (enlarged).

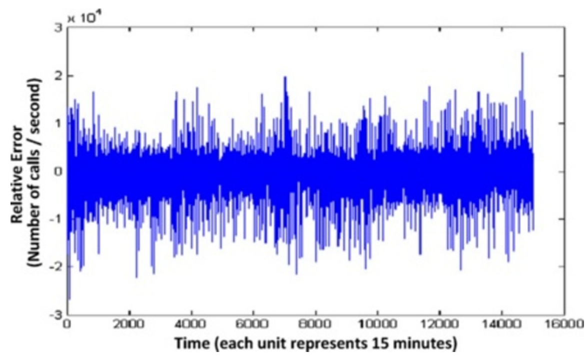

Figure 6 Relative error from training of previous half-year's data traffic load.

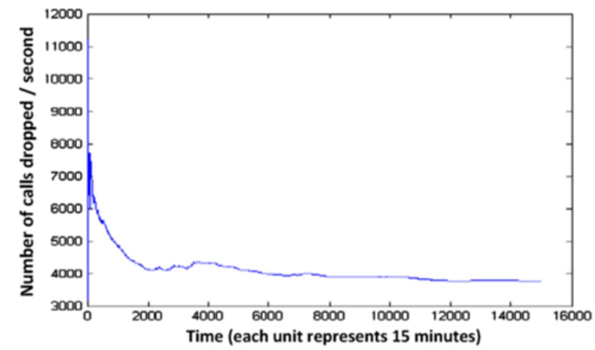

Figure 8 Rate of calls dropped from training of previous half-year's traffic load.

also vary its pilot power to dynamically change the size of the other cell. Hence, for each pair of cells, the effect is bi-directional. The dual directional interaction of cell-pairs brings to light the inevitable occurrence of coverage holes [16,19]. Assume the instance when a center cell and all its first tier neighbors are heavily loaded. At the outset, the center cell's dynamic sizing mechanism moves the boundary between the center cell and an adjacent cell inwards towards the direction of the center cell so as to allow the adjacent cells to accommodate the additional traffic in the center cell. However, due to a lack of channels in the other cell, its mechanism may instead move the boundary further away from the center cell. Thus, the dynamic cell sizing mechanisms of the two adjacent cells contradict one another. If both were to shrink simultaneously to accommodate the increasing traffic load in its own cell, coverage holes would inevitably develop, as shown in Figure 2a,b. Consequently, calls are dropped and the grade of service may not be maintained. The dual directional influence is similar for all cell pairs. Thus, coverage holes may develop between any two heavily loaded cells.

A center cell will receive dual directional impact from all cells within its first tier. Similarly, all first tier cells will also receive dual directional impact from its surrounding first tier cells. The same influence is observed in cells of subsequent tiers. Thus, a multifarious interaction of a vast number of cells is observed and this poses a high possibility of the occurrence of coverage holes [16].

2.4. Motivation for new IPCAM for dynamic cell sizing

The high incidence of coverage holes results in a large number of calls dropped. In order to mitigate the occurrence of coverage holes, a new IPCAM for dynamic cell sizing is proposed. The proposed model is an integration of two main components; the modified VC-PGA cell priority selection model and the EFuNN mobile traffic prediction model. The VC-PGA module aims to control the number of cell attenuations in a diverse cell interaction environment by ordering the priority for size attenuation of all cells within a network based on the level of mobile traffic within each cell, using two priority numbers. The EFuNN module allows for a favorable cell attenuation order by predicting the mobile traffic in advance, before congestion takes place. The EFuNN module predicts the mobile traffic volume of a particular cell by extracting

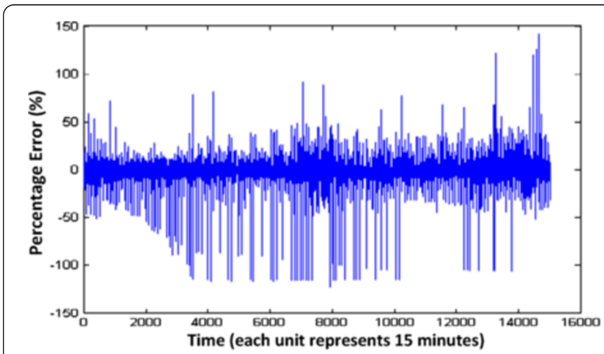

Figure 7 Percentage error from training of previous half-year's data traffic load.

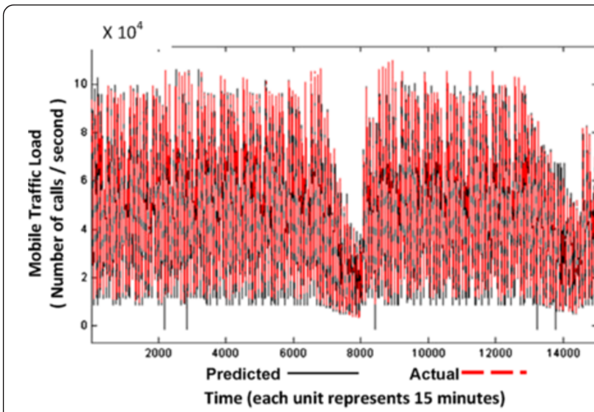

Figure 9 Prediction of the following half-year's data traffic rates based on the training of previous half-year's data traffic load.

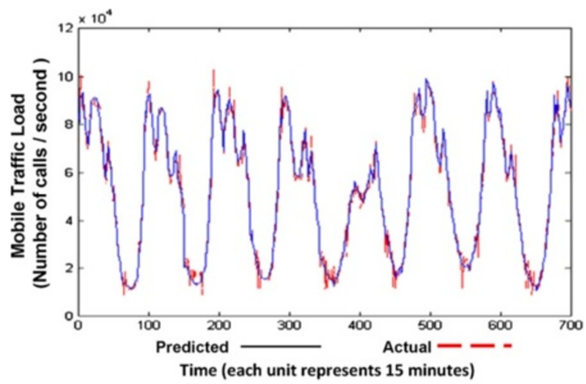

Figure 10 Prediction of the following half-year's data traffic rates based on the training of previous half-year's data traffic load (enlarged).

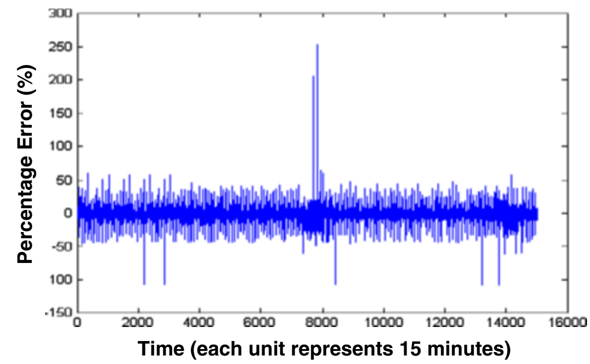

Figure 12 Percentage error from prediction of subsequent half-year's mobile traffic load.

and inserting meaningful rules through incremental, supervised real-time learning. The EFuNN module is placed in each cell and the output, the predicted mobile traffic volume of the particular cell, is sent to servers in the VC-PGA module. The VC-PGA module then assigns priorities for the size attenuation of all cells within the network, based on the predicted mobile traffic levels from the EFuNN module at each cell.

For a unified understanding of the framework and operation of the new IPCAM, it is necessary to first describe the main constituting components, as will be described in Sections 3 and 4.

3. VC-PGA module for designating cell priority for attenuation

The VC-PGA [20] has been applied for determining the cell priority for attenuation [16] and is summarized here.

First, local communities of cells and virtual communities are established, as shown in Figure 3. A local community (LC) is formed with adjacent cells, and one of the cells is elected as its local community server (LCS). Grouping LCs forms a VC. Higher-level VCs may be formed if necessary. The LCS with the highest pilot signal is elected as the virtual community server (VCS). On first run of the algorithm, any of the LCSs is arbitrarily elected as the VCS.

Then, at each LCS, the pilot powers from all cells in the LC are compared. An ordered list of pilot powers of cells within the LC is computed. The lowest pilot power is designated as the cell with the highest priority for attenuation within the LC. For other cells in the LC, the priority for size reduction will be assigned according to the ordered list of pilot power. The compliance with the local ordered list of pilot power applies only to cells whose soft handoff regions are shared with cells of the cells of same LC. Otherwise, a higher-order ordered list takes precedence. The cell with the lowest pilot power for each LC is sent to the VCS.

Meanwhile, the elected VCS will compare the pilot signal strength of received local lowest pilot signals from all LCs. The cell with the lowest pilot signal strength will have highest priority over size reduction. The hierarchy of priority for other cells will be in accordance with VC's ordered list of received local lowest pilot signal. As mentioned in Step 2, for cells whose soft handoff regions are shared with cells of a different LC, the order of

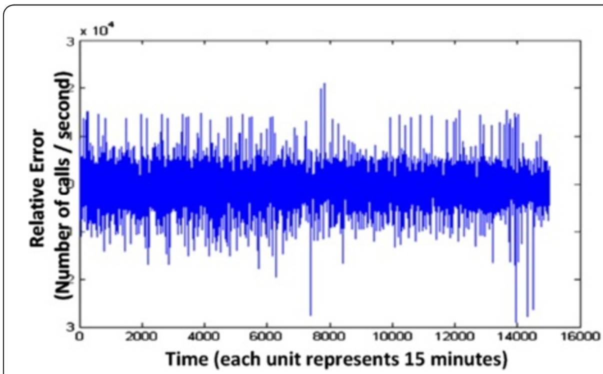

Figure 11 Relative error from prediction of the following half-year's traffic load.

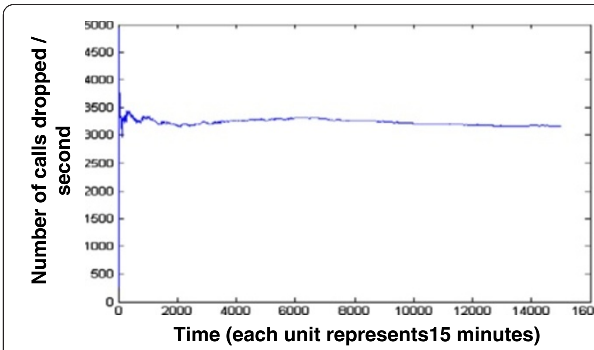

Figure 13 Number of calls dropped from prediction of subsequent half-year's data traffic load.

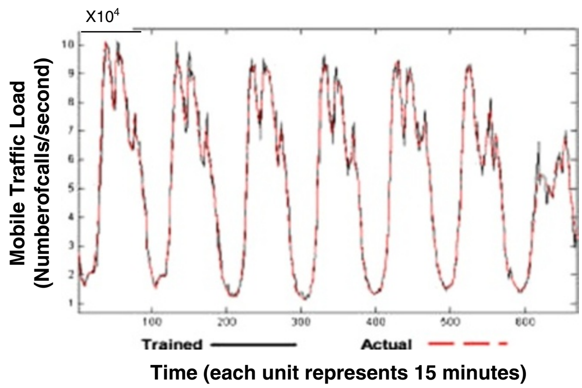

Figure 14 Training of mobile traffic load for previous week.

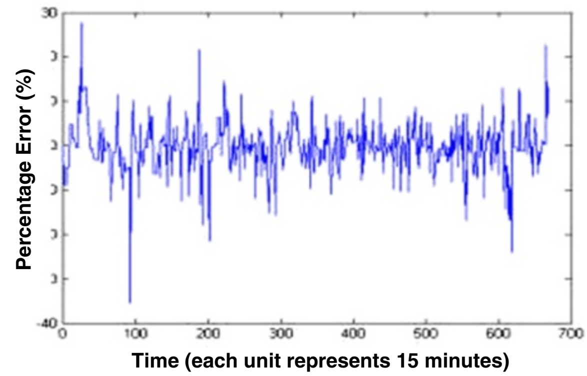

Figure 16 Percentage error from training of mobile traffic load from previous week.

precedence for cell reduction will adhere to the VC's ordered list of pilot power.

The elected cell having the lowest pilot power is broadcasted to all members of the VC. The selected cell is designated as the cell with the highest priority in cell size reduction. For cells whose soft handoff region is shared with members of the same LC, the priority for size reduction will be in accordance with the ordered list of pilot power. Otherwise, when shared with cells out of its own LC, the VC's ordered list of pilot power is adhered to. Meanwhile, the highest of all received lowest local pilot signals will be elected as the VCS for the next run as its load is the least loaded.

The advantages of VC-PGA are (i) the lowest pilot signal is obtained from a group of cell clusters in an organized manner; (ii) very little communication overhead is imposed on the mobile as information exchange is done at the LCS and VCS only; and (iii) the arrangement of cells is maintained.

4. EFuNN time-series prediction of mobile traffic volume

EFuNN was used for the prediction of future traffic volume to facilitate the selection of cell to be given the highest priority over size reduction in the proposed model due to its capabilities in adaptive, online learning. The EFuNN evolving procedure leads to a similar local online error as RAN and its modifications but EFuNNs allow for meaningful rules to be extracted and inserted at any time of the operation of the system thus providing the knowledge about the problem and reflecting changes in its dynamics. In this respect, the EFuNN is a flexible, online, knowledge engineering, and statistical model. As a statistical model, EFuNN performs clustering of the input space. The EFuNN structure also reflects the data distribution of the input–output space [12]. As an online, knowledge-based intelligent system learns quickly from a large set of data, adapts incrementally in an online mode by interacting continuously with the environment.

EFuNNs [21] adopt some known techniques from fuzzy networks and neural networks. As in fuzzy neural network, each input variable is represented by a group of spatially arranged neurons to represent a fuzzy quantization of this variable [10,12]. However, in EFuNN, the nodes representing membership functions can be modified during learning.

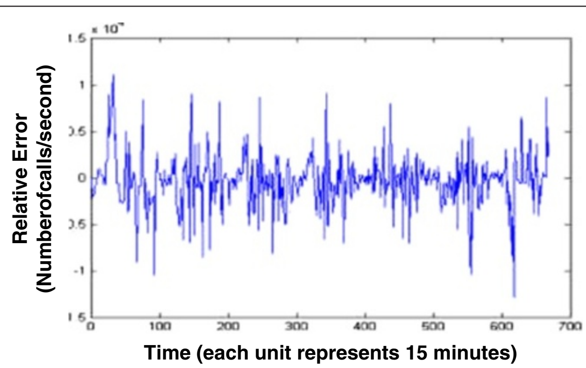

Figure 15 Relative error from training of previous week's mobile traffic load.

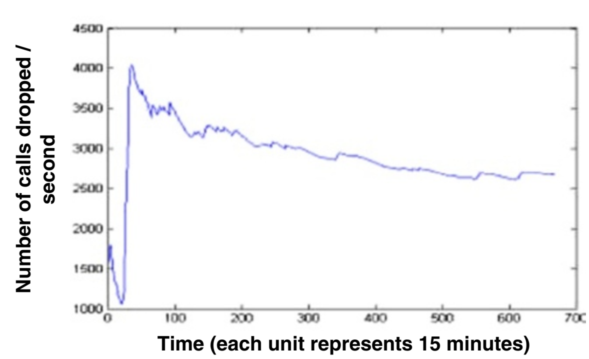

Figure 17 Rate of calls dropped for training of mobile traffic load of previous week.

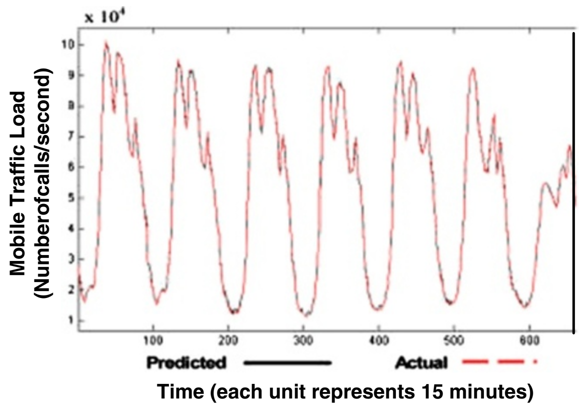

Figure 18 Prediction of mobile traffic data load for subsequent week based on training of traffic data rate for current week.

The parameter values for optimal performance for the mobile traffic data have been found as follows:

- Number of membership functions = 6
- Value for m-of-n parameter = 0.5
- Error threshold $E = 1 \times 10^{-10}$
- Maximum receptive field $R_{max} = 1$
- Rule extraction thresholds $T1$ and $T2$
- Number of examples for aggregation $N_{agg} = 4$
- Pruning parameters OLD and P_r = adaptive
- Learning rates, lr1 = lr2 = 0.9

4.1. Incorporation of traffic prediction model in VC-PGA cell priority selection model

The incorporation of the EFuNN load prediction model into the VC-PGA cell priority selection model is shown in Figure 4. This will form the IPCAM in dynamic cell sizing. The EFuNN prediction model is placed at each cell. It takes in past and current traffic volume to predict future traffic volumes. The EFuNN is flexible and online. It allows meaningful rules to be extracted and added simultaneously at any time of the operation of the system.

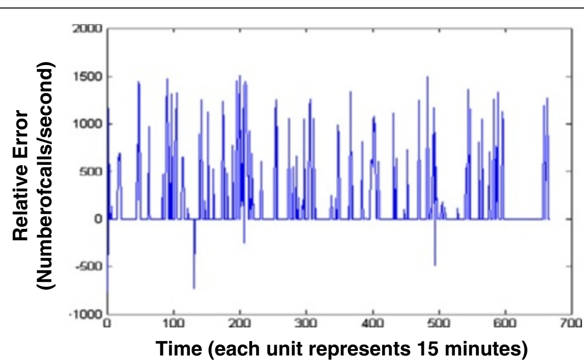

Figure 19 Relative error from prediction of mobile traffic data load for subsequent week.

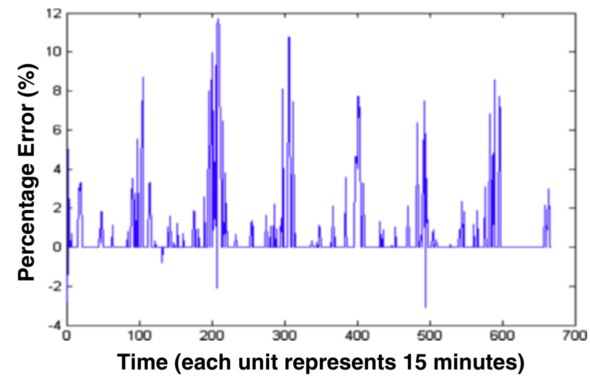

Figure 20 Percentage error from prediction of mobile traffic data load for subsequent week.

This adds knowledge on the problem and reflects changes in its dynamics. The VC-PGA cell priority selection model then takes the output from the EFuNN prediction model to select the highest-priority cell for size reduction.. It assigns a VC number and an LC number to each cell. The shrinking is then carried out according to the VC and LC numbers. This will help to resolve the problem of coverage holes and thus reduce the number of calls dropped. Retraining of the data used as input to the EFuNN traffic prediction module may be required based on preset thresholds in NDEI and RMSE values.

5. Simulation scenarios in new IPCAM

The proposed IPCAM for dynamic cell sizing in Figure 4 was developed in MATLAB. Quarter-hourly mobile traffic volume for a period of 1 year for five adjacent cells in Cyberjaya, Puchong, and Serdang in the state of Selangor was obtained courtesy of TM Touch Malaysia. Three sets of experiments to train and predict the traffic volume and number of calls dropped within the Cyberjaya cell in 15-min intervals were performed, detailed as follows:

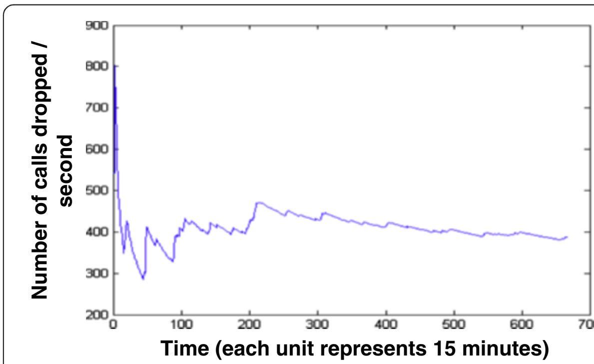

Figure 21 Number of calls dropped from prediction of mobile traffic data load for subsequent week.

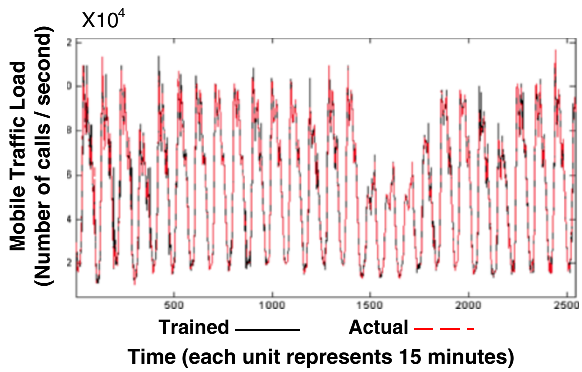

Figure 22 Training of the data traffic rates of the day before for prediction of mobile traffic data load for particular day.

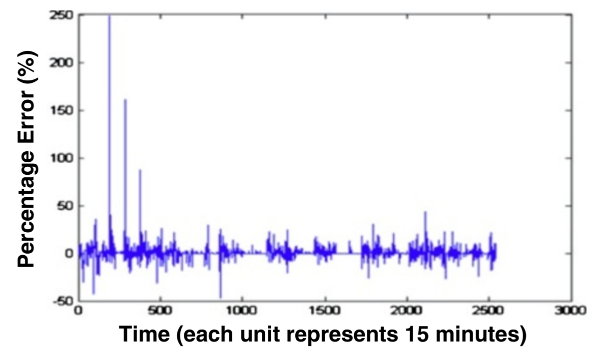

Figure 24 Percentage error from training of the data traffic load of the day before.

Set A Training of the previous half-year's data traffic rates for the prediction of the following half-year's data traffic rates.
Set B Training of the previous week's data traffic rates for the prediction of the following week's data traffic rates.
Set C Training of the data traffic rates of the day before for the prediction of the data traffic rates for the particular day.

For each experiment, the performance of the training/ prediction was evaluated by

(a) a joint graph comparing the trained/predicted value to the actual value versus time;
(b) the percentage error of the training/prediction with respect to the actual value versus time;
(c) the number of calls dropped versus time.

6. Simulation results from new IPCAM

Figures 4, 5, 6, 7, and 8 show the results for the training of previous half-year's data traffic load for the prediction of the subsequent half-year's data traffic load (Experiment A1). Figures 9, 10, 11, 12, and 13 show the results for the prediction for the subsequent half-year's data traffic load based on training of data traffic load of the first half of the year (Experiment A2). Figures 14, 15, 16, and 17 show the results for the training of the previous week's data traffic load for the prediction of the following week's data traffic load (Experiment B1). Figures 18, 19, 20, and 21 show the results for the load of the prediction of the following week's data traffic load based on the training of the previous week's data traffic (Experiment B2). Figures 22, 23, 24, and 25 show the results of the training of the data traffic load of the day before for the prediction of the data traffic load for the particular day (Experiment C1). Figures 26, 27, 28, and 29 show the results of the prediction of data traffic load for a particular day based on the training of the data traffic load of the day before (Experiment C2).

Table 1 summarizes the results for the training and prediction of all experiments. In all experiments, the general temporal pattern was recognized after some slight delay. Prediction based on previous week's data (Set B) was fastest in adapting to the pattern at the start of the simulation, followed by the prediction based on previous half-year and the day before (Set A). The best prediction results

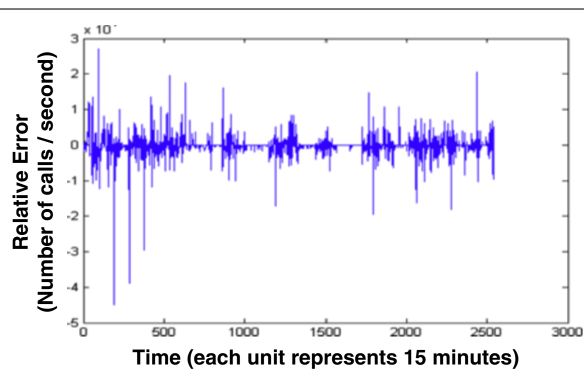

Figure 23 Relative error from training of the data traffic load of the day before.

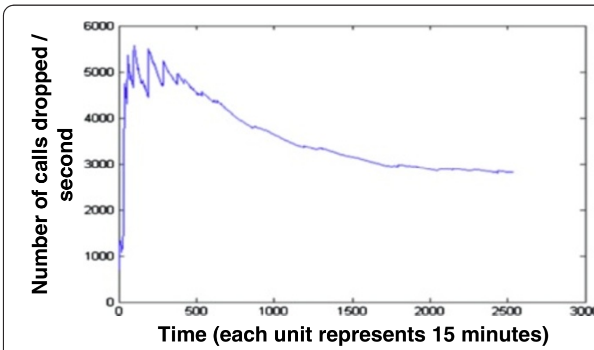

Figure 25 Number of calls dropped for training of the data traffic load of the day before.

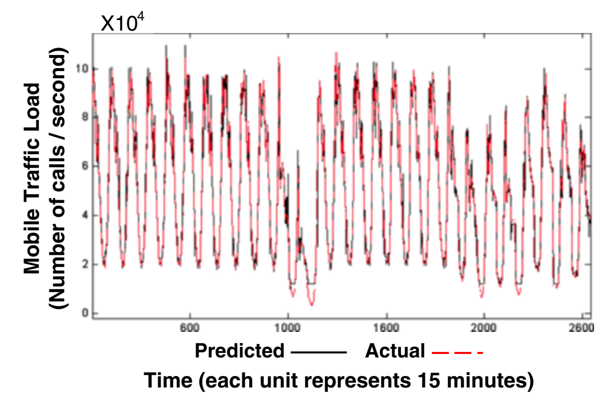

Figure 26 Prediction of mobile traffic data load for particular day based on the training of the data traffic of the day before.

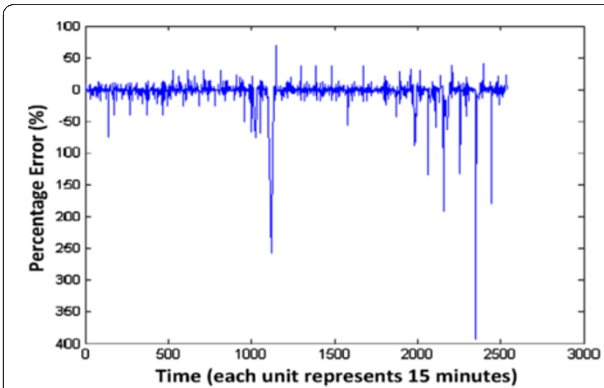

Figure 28 Percentage error from prediction of mobile traffic data load for subsequent day.

in all aspects (percentage error, time taken to adapt to pattern, number of calls dropped) were obtained when training was based on the previous week's data (Set B). Prediction results were better when only peaks were considered.

Slight fluctuations in the patterns caused delay in adapting to the changes. This occurred during festive seasons and the local university's semester breaks. The prediction errors were only slight when the earlier week's data were used (0–12%) but more severe when previous half-year's data and consecutive weeks of particular data were used (0–120 and 0–400%, respectively). The quick adaptation to pattern changes in the prediction based on prior week's data was most probably due to the close correlation between the two dataset of 1-week apart. Previous half-year's data performed less favorably as trends in mobile sales and usage would have affected the population of mobile users. Furthermore, same festivities fall slightly before or after the same day the subsequent year. On the other hand, the leap from 1 day of the week to the same day in the subsequent week is most likely to cause a discontinuity in the prediction of ongoing trends.

The VC-PGA model will take in the highest values of predicted traffic from all cells in the LC. For this reason, only evaluation at peaks will be considered. Once again, as in the overall evaluation, the prediction based on the previous week's data gives the best results at peaks. The percentage error is only 0–2%, as compared to 0–200% for prediction based on previous half-year's data and 0–400% for prediction based on subsequent consecutive weeks of particular day. Therefore, the VC-PGA model will run based on prediction using training data of previous week. The VC-PGA model takes in the highest values of predicted traffic from all cells in the LC. For this reason, only evaluation at peaks is significant. Once again, as in the overall evaluation, the prediction based on the previous week's data gives the best results at peaks. Most importantly, the number of calls dropped was shown to decrease for all experiments. The percentage decrease in the number of calls dropped was largest for Experiments 3 and 4. Thus, assuming a large portion of calls dropped is due to coverage holes, it has been proven that the proposed model controls cell attenuation efficiently to reduce the number of calls dropped.

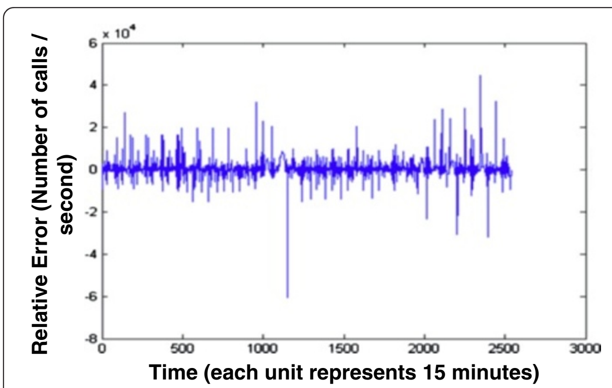

Figure 27 Relative error from training of mobile traffic data load for particular day.

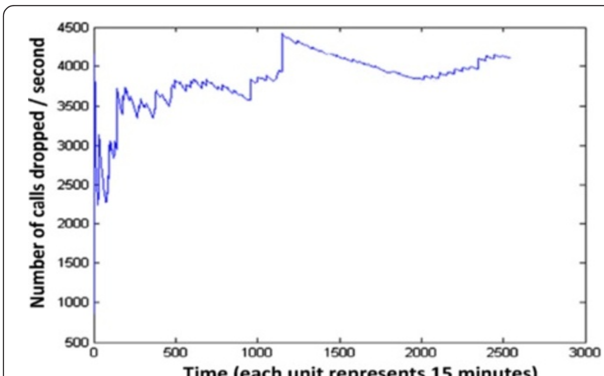

Figure 29 Number of calls dropped from prediction of mobile traffic data load for subsequent day.

Table 1 Summary of training and prediction results for all experiments

Experiment		Relative error (range)	% Error (%)	% Error at peaks (%)	Rate of calls dropped (starting)	Rate of calls dropped (ending)
A1	Training of previous half-year's data	0 to 2.8×10^4	0–120	7800	3900	0–120
A2	Prediction of subsequent half-year's data	0–2.8×10^4	0–200	3750	3200	0–200
B1	Training of previous week's data	0–1.3×10^4	0–28	4000	2700	0–12
B2	Prediction of subsequent week's data	0–1495	0–12	800	400	0–2
C1	Training of previous consecutive weeks of particular day	0–4.5×10^4	0–50 (but starts at 0–250)	5500	3000	0–50 (but starts at 0–250)
C2	Prediction of subsequent consecutive weeks of particular day	0–6.0×10^4	0–400	3000	4000	0–400

7. Conclusions

A new, robust IPCAM in dynamic cell sizing is proposed and simulated using real mobile traffic data in Selangor, Malaysia. The proposed model is an integration of two main components, namely the VC-PGA cell priority selection model and the EFuNN mobile traffic prediction module. The VC-PGA module successfully controlled the number of cell attenuations in a diverse cell interaction environment based on two cell priority numbers and reduced the number of calls dropped. The EFuNN module, placed at each cell, predicted the mobile traffic volume of a particular cell by extracting and inserting meaningful rules through incremental, supervised real-time learning. The output of the EFuNN structure from each cell, the predicted mobile traffic volume of the particular cell, was delivered to servers in the VC-PGA module and the priorities for the size reduction of all cells were assigned.

The performance of the proposed model was evaluated on five adjacent cells in Selangor, Malaysia. Experiments to evaluate the robustness of the integrated model in controlling the cell size to reduce the number of calls dropped were conducted. Real-time predicted mobile traffic from the EFuNN structure was used to control the size of all the cells within 15-min intervals. The mobile traffic was predicted based on the data of five adjacent cells consisting of data from the (1) previous half-year, (2) previous week, (3) same day of the previous week. The results for each experiment, for both training and prediction, were evaluated in terms of the predicted traffic volume and the number of calls dropped.

Results obtained demonstrate the robustness of the integrated model in recognizing the general temporal patterns of traffic and controlling the number of calls dropped. The proposed model controlled cell attenuations under various local traffic conditions throughout the year. The least number of calls dropped were achieved when the prediction was based on training of traffic load from the previous week.

Competing interests
The authors declare that they have no competing interests.

Acknowledgments
The authors would like to thank Celcom Malaysia for providing traffic data in Selangor, Malaysia.

Received: 3 April 2012 Accepted: 31 October 2012
Published: 27 November 2012

References

1. JMR Aviles, S Luna-Ramirez, M Toril, F Ruiz, I de la Bandera-Cascales, P Munoz-Luengo, Analysis of load sharing techniques in enterprise LTE femtocells, in Wirel. Adv. (WiAd), 195–200 (2011). 20-22 June 2011, London, UK
2. H Kim, G de Veciana, X Yang, M Venkatachalam, Alpha-optimal user association and cell load balancing in wireless networks, in *Proceedings IEEE 2010 INFOCOM'2010* (San Diego, 2010), pp. 1–5
3. H Wang, L Ding, P Wu, Z Pan, N Liu, X You, Dynamic load balancing in 3GPP LTE multi-cell networks with heterogenous services, in *5th International ICST Conference on Communications and Networking in China (CHINACOM)*, ed. by (Beijing, China, 2010), pp. 1–5
4. F Xiang, H Xiaoyan, L Junzhou, W Jieyi, G Guanqun, Fuzzy neural network based traffic prediction and congestion control in high-speed networks. J. Comput. Sci. Technol. **15**, 144–149 (2008)
5. M Salem, A Adinoyi, M Rahman, H Yanikomeroglu, D Falconer, Y-D Kim, Fairness-aware radio resource management in downlink OFDMA cellular relay networks. IEEE Trans. Wirel. Commun. **9**, 1628–1639 (2010)
6. J Shapiro, D Towsley, J Kurose, Optimization-based congestion control for multicast communications. IEEE Commun. Mag. **40**, 90–95 (2002)
7. IE Khayat, P Geurts, G Leduc, Enhancement of TCP over wired/wireless networks with packet loss classifiers inferred by supervised learning. Wirel. Netw. **16**, 273–290 (2010)
8. OA Ojesanmi, A Ojesanmi, O Makinde, Development of prioritized handoff scheme for congestion control in multimedia wireless network, in *Proceedings of the World Congress on Engineering (WCE)*, ed. by (London, U.K., 2009), pp. 895–900
9. P Soldati, B Johansson, M Johansson, Distributed cross-layer coordination of congestion control and resource allocation in S-TDMA wireless networks. Wirel. Netw. **14**, 949–965 (2008)
10. Y Bejerano, S-J Han, Cell breathing techniques for load balancing in wireless LANs. IEEE Trans. Mob. Comput. **8**, 735–749 (2009)
11. P Bahl, MT Hajiaghayi, K Jain, V Mirrokni, L Qiu, A Saberi, Cell breathing in wireless LANs: algorithms and evaluation. IEEE Trans. Mob. Comput. **6**, 164–178 (2007)
12. K Jain, P Bahl, L Qiu, V Mirrokni, M Hajiaghayi, A Saberi, *Wireless LAN cell breathing* (2010). Patent 7715353
13. S-W Wong, LG Kazovsky, Y Yan, L Dittmann, MPCP Assisted Power Control and Performance of Cell Breathing in Integrated EPON-WiMAX Network, in *Global Telecommunications Conference 2009 (GLOBECOM 2009)*, ed. by (IEEE Honolulu, USA, 2009), pp. 1–6
14. JM Kelif, M Coupechoux, Cell breathing, sectorization and densification in cellular networks, in *7th International Symposium on Modeling and*

Optimization in Mobile, Ad Hoc, and Wireless Networks, 2009 (WiOPT 2009) (Seoul, 2009), pp. 1–7
15. E Garcia, R Vidal, J Paradells, Cooperative load balancing in IEEE 802.11 networks with cell breathing, in *IEEE Symposium on Computers and Communications, 2008 (ISCC 2008)*, ed. by (Marrakech, Morocco, 2008), pp. 1133–1140
16. A Amphawan, EM Abraham, Diverse Cell Interactions in Dynamic Cell Sizing and VC-PGA Cell Priority Selection Method, in *IEEE Proceedings of the Eighth IEEE International Conference on Communications Systems (ICCS 2002)* (Singapore, 2002), pp. 459–463
17. A Amphawan, EM Abraham, R Govindaraju, Cell Breathing in CDMA Networks, in *Second International Symposium on Communications and Information Technology (ISCIT 2002)*, ed. by (Pattaya, Thailand, 2002), pp. 21–24
18. A Jalali, On Cell Breathing in CDMA Networks, in *IEEE International Conference on Communications*, ed. by (Atlanta, 1998), pp. 985–988
19. A Amphawan, EM Abraham, Dynamic cell sizing in CDMA Networks. Information Technology Journal **1**(3), 264–268 (2002)
20. N Kasabov, T Yamakwa, G Matsumoto, Evolving fuzzy neural networks—algorithms, applications and biological motivation, in *Methodologies for the Conception, Design and Application of Soft Computing (World Scientific, Singapore, 1998)*, ed. by, pp. 422–425
21. L Tan, D Taniar, KA Smith, A new parallel genetic algorithm, in *Proceedings of the International Symposium on Parallel Architectures, Algorithms and Networks (ISPAN)*, ed. by, 2nd edn. (Makati City, 2002), pp. 284–289

doi:10.1186/1687-1499-2012-356
Cite this article as: Amphawan *et al.*: An integrated priority-based cell attenuation model for dynamic cell sizing. *EURASIP Journal on Wireless Communications and Networking* 2012 **2012**:356.

Submit your manuscript to a SpringerOpen journal and benefit from:

- ► Convenient online submission
- ► Rigorous peer review
- ► Immediate publication on acceptance
- ► Open access: articles freely available online
- ► High visibility within the field
- ► Retaining the copyright to your article

Submit your next manuscript at ► springeropen.com